Back to Session Subjects

A COMPARISON AMONG SOME AEROELASTIC MODELS FOR THE STABILITY ANALYSIS OF A FLAP-LAG-TORSION HELICOPTER ROTOR IN HOVER

M. Gennaretti‡, A. Corbelli*, F. Mastroddi*

‡University Roma Tre
Dipartimento di Ingegneria Meccanica e Industriale
via della Vasca Navale 79 - 00146 Rome, Italy
e-mail: m.gennaretti@uniroma3.it

*University of Rome 'La Sapienza'
Dipartimento Aerospaziale, Rome, Italy

Abstract

The aim of this paper is the aeroelastic analysis of a hovering-rotor cantilever blade in flap-lag-torsion motion, with emphasis on the unsteady aerodynamics modeling. The structural dynamics is described by a nonlinear integro-partial differential system of equations, whereas the aerodynamic load prediction is obtained by applying both two-dimensional analytical models and three-dimensional models based on a frequency-domain boundary-element solution. The aeroelastic analysis is performed by first applying the Galërkin approach for the space integration, and then solving the eigenproblem obtained by linearization of the resulting ordinary-differential equations about the steady equilibrium operating conditions. Numerical investigation is focused on comparison among aeroelastic predictions obtained from different aerodynamic modelings, and on analysis of the aeroelastic damping of a two-bladed, hovering rotor for different values of collective pitch and precone angle, for which experimental data are available.

1 Introduction

The subject of this work is the aeroelastic stability analysis of a hovering helicopter rotor. This analysis is specifically addressed to the identification of the most critical aspects in modeling the aeroelastic behavior, with emphasis on the unsteady aerodynamics. Indeed, the simulation of aeroelastic behavior of a helicopter rotor is not a simple task, and particular attention must be paid on the formulation of the mathematical models describing all physical phenomena involved in the fluid-structure interaction.

In the last decades, several aerodynamic models have been applied to the aeroelastic analysis of rotors. Lots of them are based on the two-dimensional analytical solution introduced by Loewy [1], or on its quasi-steady version that assures a considerable simplification of the resolution algorithm. Some others have developed more accurate fully three-dimensional models, like those reviewed in Ref.[2] or that presented in Ref. [3]. Each approach has advantages and disadvantages, and the best choice depends on the problem to be analysed, and the required accuracy. Here, we wish to compare the capability of different aerodynamic approaches, some based on analytical solutions, some others based on a frequency-domain boundary element method (BEM), to capture the aeroelastic behavior of a flap-lag-torsion blade hovering rotor.

The aim of the numerical investigation is twofold. First, we intend to analyse the differences induced in the predicted aeroelastic stability, by the use of the different aerodynamic models mentioned above. Specifically, we investigate about differences in aeroelastic prediction between formulations based on two-dimensional and three-dimensional aerodynamic models, Furthermore, within the two-dimensional aerodynamic approaches, and the three-dimensional approaches, we analyse also the decrease of solution accuracy induced by the (simplifying) adoption of low or very-low frequency approximations. Second, we compare our numerical results with experimental data presented in [**?**], that concerns the aeroelastic damping of a two-bladed, hovering rotor for different values of collective pitch and precone angle.

2 Blade Structural Model

In this work, aeroelastic models for rotor blades have been derived by using the nonlinear flap-lag-torsion equations of motion presented by Hodges

and Ormiston [5], and derived by simplifying the more general beam-like blade model, introduced by Hodges and Dowell [6], that is valid for twisted, nonuniform blades, with both mass and tensile offsets.
In the equations of motion given in Ref. [5], the blade is assumed to be untwisted with uniform distribution of mass, and with mass, tensile and aerodynamic axes coinciding with the elastic axis. In deriving the final form of these equations, they have been further manipulated. First, an ordering scheme has been applied in order to drop those terms considered to be of the third order with respect to the bending slope (an arbitrary small parameter), and not contributing to damping. Second, the radial displacement of the blade has been eliminated from the system of equations, by solving it in terms of local tension: this is equivalent to assume that the blade is inextensible for bending deflections, and that radial displacements are simply geometric consequences of the transverse bending deflections (see Ref. [5] for details).
Under all the simplifying assumptions mentioned above, the final form of the system of equations governing the blade structural dynamics, is a set of coupled integro-partial differential equations having as unknowns the lateral in-plane displacement of the elastic axis, $v(x,t)$, the lateral out-of-plane displacement of the elastic axis, $w(x,t)$, and the cross-section elastic torsion deflection $\varphi(x,t)$. Addressing the reader to Ref. [5] for their complete expressions, the blade equations of motion may be synthetized in the following form:

$$m\,\ddot{v} + \mathcal{O}_v[v,w,\varphi,\dot{v},\dot{w}] = \mathcal{L}_v \qquad (1)$$

$$m\,\ddot{w} + \mathcal{O}_w[v,w,\varphi,\dot{v},\dot{w}] = \mathcal{L}_w \qquad (2)$$

$$J_\varphi\,\ddot{\varphi} + \mathcal{O}_\varphi[v,w,\varphi] = \mathcal{M}_\varphi, \qquad (3)$$

where m denotes the blade mass per unit length, J_φ denotes the cross-section torsional mass moment of inertia, $\mathcal{O}_v$ and $\mathcal{O}_w$ denote fourth-order in space, nonlinear, integro-partial differential operators, whereas $\mathcal{O}_\varphi$ denotes a second-order in space, nonlinear, partial differential operator. Furthermore, $\mathcal{L}_v$ and $\mathcal{L}_w$ are, respectively, the in-plane and out-of-plane aerodynamic forces per unit length acting on the blade, whereas $\mathcal{M}_\varphi$ is the aerodynamic pitching moment per unit length acting on the blade.
Due to the complexity of the aerodynamic field generated by rotor blade motion, the derivation of an accurate model for the prediction of the aerodynamic loadings appearing in equations (1)–(3) is not an easy task, and will be discussed in the next section and in Appendices B and C. In the following, we describe the approach adopted for the integration of the set of equations of motion for the aeroelastic analysis of hovering rotors.

3 Modal-Approach Solution

The solution of the set of coupled integro-partial differential equations (1)–(3), has been obtained by following the approach presented in [5] for a hingeless rotor blade. It is based on the application of the Galërkin method for the spatial integration of the equations, followed by the definition of two separate problems: a nonlinear algebraic problem for the evaluation of equilibrium stationary blade deflections, and a linear time-differential problem with unknown the perturbations of blade deflections with respect to the evaluated equilibrium condition (typical linear stability analysis procedure).
Specifically, first the elastic blade deflections have been expressed in terms of the following series

$$v(x,t) = \sum_{n=1}^{N} q_n^v(t)\,\Psi_n^v(x) \qquad (4)$$

$$w(x,t) = \sum_{n=1}^{N} q_n^w(t)\,\Psi_n^w(x) \qquad (5)$$

$$\varphi(x,t) = \sum_{n=1}^{N} q_n^\varphi(t)\,\Psi_n^\varphi(x), \qquad (6)$$

where $\Psi_n^v, \Psi_n^w, \Psi_n^\varphi$ are sets of linearly independent shape functions (mode shapes), whereas $q_n^v, q_n^w, q_n^\varphi$ denote the generalized coordinates of the problem (modal amplitudes). Considering that the rotor analysed in this work (see Section 5) consists of two hingeless blades, the mode shapes appearing in equations (4)–(6), have been chosen to be the (analytical) eigenfunctions of the cantilever nonrotating beam.
Next, substituting equations (4)-(6) into equations (1)–(3), the Galërkin method yields a set of $3N$ nonlinear, ordinary differential (modal) equations in terms of the generalized coordinates of the problem. In order to define the equilibrium-configuration and perturbation problems mentioned above, it is convenient to introduce the following expressions

$$q_n^v(t) = q_{0n}^v + \Delta q_n^v(t) \qquad (7)$$

$$q_n^w(t) = q_{0n}^w + \Delta q_n^w(t) \qquad (8)$$

$$q_n^\varphi(t) = q_{0n}^\varphi + \Delta q_n^\varphi(t), \qquad (9)$$

where the q_{0n}'s denote steady equilibrium values, whereas the Δq_n's denote small perturbations. Substituting the steady equilibrium values into the modal nonlinear differential equations obtained through application of the Galërkin method, one obtains the first set of $3N$ nonlinear algebraic equations, with unknown the equilibrium modal amplitudes $q_{0n}^v, q_{0n}^w, q_{0n}^\varphi$. Then, substituting equations (7)–(9) into the nonlinear differential modal equations, subtracting the steady

equilibrium equations and dropping all (nonlinear) terms containing products of the perturbation quantities, one obtains a set of linear ordinary differential equations, with coefficients depending on the steady equilibrium values of the modal amplitudes, that may be recast in the following form

$$\mathsf{M}(\mathsf{q}_0)\ddot{\mathsf{q}} + \mathsf{C}(\mathsf{q}_0)\dot{\mathsf{q}} + \mathsf{K}(\mathsf{q}_0)\mathsf{q} = \mathsf{f}_A(\mathsf{q}_0, \ddot{\mathsf{q}}, \dot{\mathsf{q}}, \mathsf{q}, t), \quad (10)$$

where q is a vector of length $3N$ containing the perturbation modal amplitudes $\Delta q_n^v, \Delta q_n^w, \Delta q_n^\varphi$, $\mathsf{M}, \mathsf{C}, \mathsf{K}$ are the inertial-structural mass, damping and stiffness matrices depending on the equilibrium solution, q_0, whereas f_A is a vector containing the generalized aerodynamic forces, *i.e.,* those forces obtained by projecting $\mathcal{L}_v, \mathcal{L}_w, \mathcal{M}_\varphi$ of equations (1)–(3), onto the mode shapes of equations (4)-(6), as indicated by the Galërkin method.

4 Stability Analysis

Once the equilibrium configuration has been determined, the stability analysis may be accomplished by analysing the behavior of the solution obtained integrating equation (10). However, if a linear aerodynamic model is available for expressing f_A as an explicit function of the perturbations q, the most convenient approach for the stability analysis is that based on the solution of the eigenproblem, that directly yields the damping characteristics of the system. Indeed, assuming that (see next section) the generalized aerodynamic forces are expressed by a linear combination of the perturbation variables, in the frequency domain we have

$$\tilde{\mathsf{f}}_A(s) = \mathsf{E}(\mathsf{q}_0, s)\,\tilde{\mathsf{q}}, \quad (11)$$

with E the equilibrium-dependent matrix containing the $3N \times 3N$ transfer functions between perturbation variables and generalized aerodynamic forces. Therefore, transforming equation (10) into frequency domain and combining with equation (11), one obtains the following eigenproblem

$$[s^2\,\mathsf{M}(\mathsf{q}_0) + s\,\mathsf{C}(\mathsf{q}_0) + \mathsf{K}(\mathsf{q}_0) - \mathsf{E}(\mathsf{q}_0, s)]\,\tilde{\mathsf{q}} = 0, \quad (12)$$

whose eigenvalues describe the aeroelastic behavior of the structure (in the following, for simplicity of notation, the dependence of E on q_0 will be assumed implicitly).

Of course, the complexity of the aerodynamic transfer functions included in matrix E depends on the model chosen to predict the aerodynamic solution. However, due to the unsteadiness of the flow, and in particular of the wake vorticity, analytical models based on the two-dimensional solution introduced by Loewy [1], indicate that if a low-frequency approximation is not applied, these transfer functions are transcendental functions of the frequency (see next section). In this case, the eigenproblem (12) has an infinite number of eigenvalues, and the determination of the aeroelastic behavior through the eigenproblem solution is no more convenient (unless only the stability margins are required, so that a 'p-k' approach is applicable). Therefore, in this work, when using an aerodynamic model introducing frequency transcendental transfer functions (namely, the Loewy-Greenberg formulation and the BEM approach discussed in Appendices B and C, respectively), we approximate the matrix E, by a rational-matrix expression of the type (see Appendix A, equation (18)),

$$\mathsf{E}(s) \approx s^2\,\mathsf{A}_2 + s\,\mathsf{A}_1 + \mathsf{A}_0 + \mathsf{H}\,[s\,\mathsf{I} - \mathsf{G}]^{-1}\,\mathsf{F}, \quad (13)$$

where $\mathsf{A}_2, \mathsf{A}_1, \mathsf{A}_0, \mathsf{H}, \mathsf{G}, \mathsf{F}$ are constant matrices evaluated by the least-square technique presented in Ref. [7], and briefly outlined in Appendix A. Indeed, substituting equation (14) in equation (12), and introducing a new vector

$$\tilde{\mathsf{r}} = [s\,\mathsf{I} - \mathsf{G}]^{-1}\,\mathsf{F}\,\mathsf{q}, \quad (14)$$

whose dimensions depend on the dimensions of the matrix G, the aeroelastic eigenproblem may be recast in the following form

$$[s^2\,\hat{\mathsf{M}}(\mathsf{q}_0) + s\,\hat{\mathsf{C}}(\mathsf{q}_0) + \hat{\mathsf{K}}(\mathsf{q}_0)]\,\tilde{\mathsf{x}} = 0, \quad (15)$$

with

$$\hat{\mathsf{M}} = \begin{bmatrix} \mathsf{M} - \mathsf{A}_2 & 0 \\ 0 & 0 \end{bmatrix}, \quad \hat{\mathsf{C}} = \begin{bmatrix} \mathsf{C} - \mathsf{A}_1 & 0 \\ 0 & \mathsf{I} \end{bmatrix},$$

$$\hat{\mathsf{K}} = \begin{bmatrix} \mathsf{K} - \mathsf{A}_0 & -\mathsf{H} \\ -\mathsf{F} & -\mathsf{G} \end{bmatrix},$$

and the vector $\mathsf{x}^T = \left\{\mathsf{q}^T, \mathsf{r}^T\right\}$, containing the modal perturbation variables, q, and the additional variables, r, arising from the matrix-fraction approximation of the aerodynamic matrix. Now, the aeroelastic eigenproblem expressed in equation (15) has a finite number of eigenvalues (depending on the number of the additional states required), and therefore it is possible to determine the damping characteristics of all of the states of the system and, in the event, the aeroelastic response to an external perturbation like, *e.g.,* an atmospheric gust.

Note that, operating in the way described above means to describe explicitly the aerodynamic loads by a number of states, that is greater than that needed for the description of the structural dynamics. Indeed, combining equation (11) with equation (14), in time domain one obtains

$$\mathsf{f}_A(t) = \mathsf{A}_2\,\ddot{\mathsf{q}} + \mathsf{A}_1\,\dot{\mathsf{q}} + \mathsf{A}_0\,\mathsf{q} + \mathsf{H}\,\mathsf{r},$$

with $\dot{\mathsf{r}} = \mathsf{G}\,\mathsf{r} + \mathsf{F}\,\mathsf{q}$. This is due to the fact that for the evaluation of the time evolution of a mechanical structure you only need to know its current state and velocity, whereas the flow field on a lifting body is influenced also by the vorticity generated by the body, and hence has 'memory' of the past flow evolution.

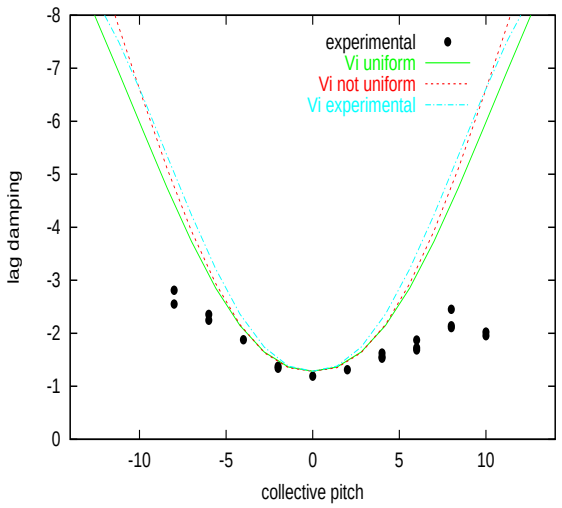

Figure 1: lead-lag damping from quasi-steady aerodynamics, using three induced velocity models. $\beta = 0°$.

Finally, note also that transforming equation (15) back into time domain, one obtains a system of constant-coefficient ordinary differential equations describing the aeroelastic system, that may be conveniently applied for aeroservoelastic purposes.

5 Numerical Results

In this work, the aeroelastic formulation presented above has been applied to the evaluation of the lead-lag damping of the hovering rotor investigated in Ref. [4]. This is a two bladed, hingeless, untwisted rotor, with radius $R = 0.9615$m, constant chord $c = 0.0864$m, and NACA 0012 section airfoil (for the detailed description of the structural characteristics of the blades, see Ref. [4]).

First, we have considered the case with precone angle $\beta = 0°$, and rotor angular velocity $RPM = 1000$ (for all the results presented in the following, we have considered this value of the angular velocity). In Figure 1 we present the comparison among the measured lead-lag damping given in Ref. [4], and those computed using the (very) low-frequency approximation of the Loewy-Greenberg formulation, $\mathcal{C}_L = 1$ (quasi-steady aerodynamics), with three different models for the induced velocity, v_i.

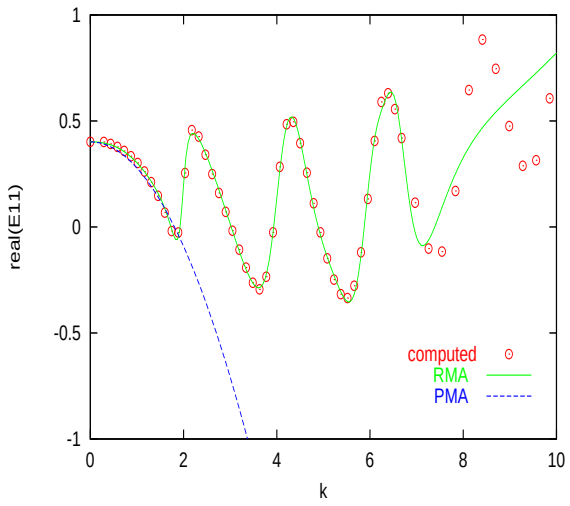

Figure 2: real part of E_{11} from the Loewy-Greenberg formulation.

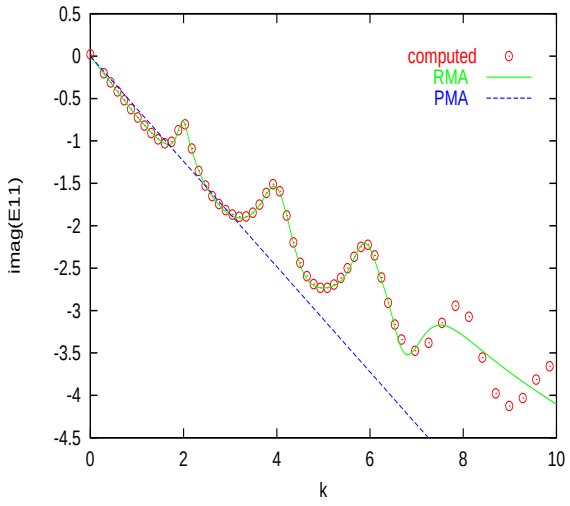

Figure 3: imaginary part of E_{11} from the Loewy-Greenberg formulation.

Specifically, we have applied uniform-inflow and non-uniform-inflow models based on a combination of blade element and momentum theory (see, *e.g.*, Ref. 8]), with the addition of an empirical model based on the experimental results given in Ref. [4]. As illustrated in Figure 1, these three models give damping predictions that appear to be very similar for the whole range of collective pitch angle considered. All of them are in good agreement with the experimental data for small values of the pitch angle, but the agreement rapidly decreases for increased pitch angles. This might be due to the fact that as the pitch angle increases, more and more important is the role of the aerodynamic loads on the aeroelastic behavior. Therefore, in this range of collective pitch, these very simple aerodynamic models do not predict unsteady loads with satisfactory ac-

curacy, also when using a realistic distribution of induced velocity.

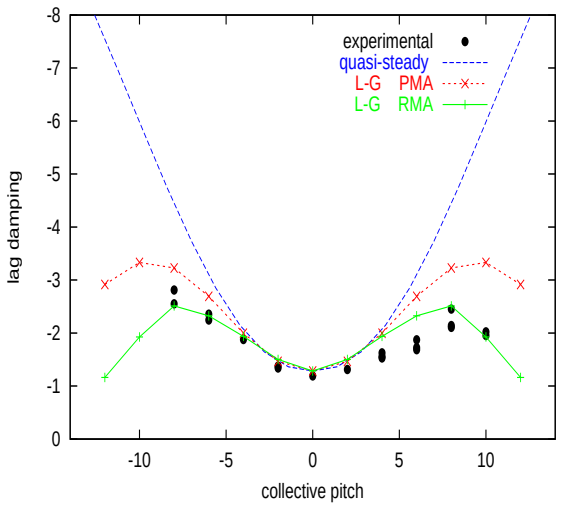

Figure 4: lead-lag damping from the Loewy-Greenberg formulation using three induced velocity models. $\beta = 0°$.

Next, we have considered the aerodynamic model based on the Loewy-Greenberg formulation. In this case, as explained in Section 4, we have approximated the aerodynamic matrix by the least-square-approximation technique outlined in Appendix A. However, this technique has been applied in two different ways: the first consists of requiring an accurate approximation of the aerodynamic transfer functions only in a low range of the reduced frequency, k, (in this case, $k \leq 2$), whereas the second extends the requirement up to $k = 7$, and for greater values requires only the mean value to be satisfactorily approximated. The relevant difference between these two approaches consists in the fact that for the (weakly) low-frequency approximation of the aerodynamic matrix, a simple frequency quadratic form may be used (it is indicated as PMA -polynomial matrix approximation- in the following), that does not contain poles, and hence does not generate additional aerodynamic states for the aeroelastic system, whereas the second approach requires the inclusion of a lot of additional states (RMA -rational matrix approximation- in the following). The approximations obtained following the two approaches are illustrated in Figures 2 and 3, taking into consideration the first element of the aerodynamic matrix, for $\theta = 12°$. As expected, the low-frequency approximation differs considerably from the computed values for high values of the collective pitch; however, its approximation is similar to that of the more accurate approach for $k \leq 2$. Of course, the effects of these differences on the aeroelastic solution are not relevant if the values of the most important characteristic frequencies of the system are included in the low frequency range considered (note that using the more accurate approximation shown in Figures 2 and 3, 24 additional states must be included in the aeroelastic system).

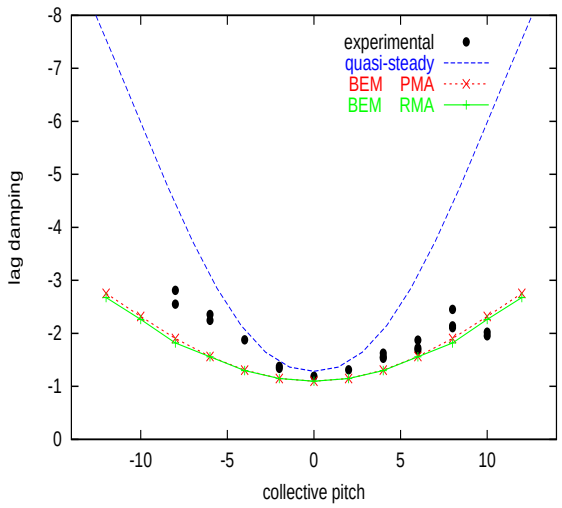

Figure 5: lead-lag damping from BEM formulation using three induced velocity models. $\beta = 0°$.

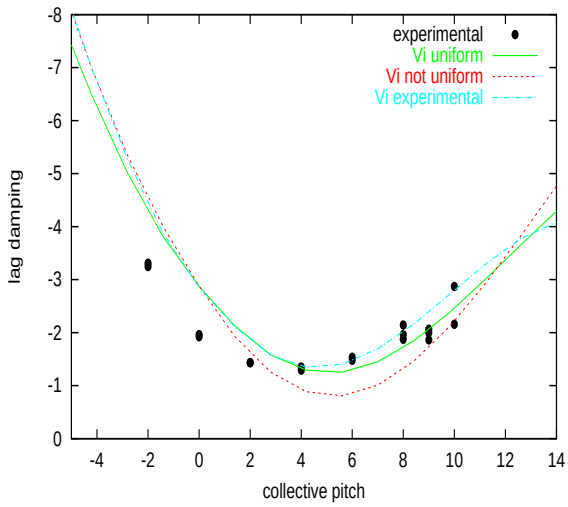

Figure 6: lead-lag damping from quasi-steady aerodynamics, using three induced velocity models. $\beta = 5°$.

Then, Figure 4 shows the lead-lag damping predicted with these two aerodynamic models based on the Loewy-Greenberg formulation. The accuracy of these results is much better than that obtained from the quasi-steady aerodynamics, in particular for large values of the collective pitch angle. The low frequency approximation demonstrates to give very satisfactorily results, in particular in consideration of the simplicity of the expression used for its approximation, and of the absence of additional states. Finally, for the case

with $\beta = 0°$, Figure 5 shows results that are equivalent to those presented in Figure 4, but obtained by the BEM aerodynamic solution. In this case, the numerical solution is in very good agreement with the experimental results, both using the PMA approach and using the RMA one.

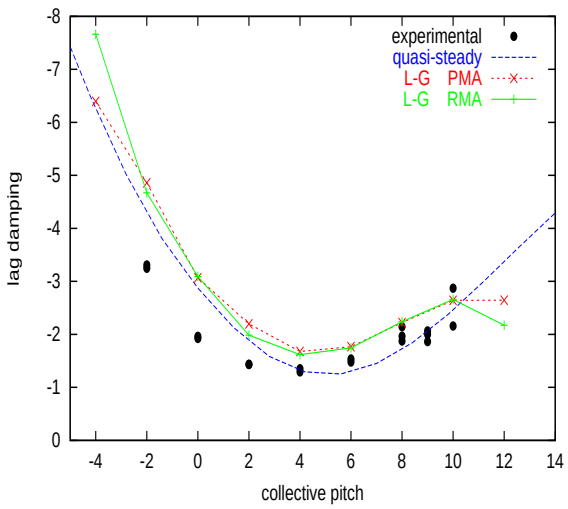

Figure 7: lead-lag damping from the Loewy-Greenberg formulation using three induced velocity models. $\beta = 5°$.

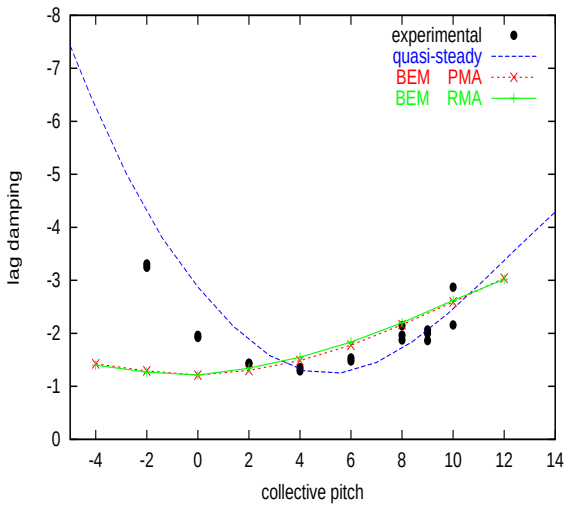

Figure 8: lag damping from BEM formulation using three induced velocity models. $\beta = 5°$.

Next, the same analysis has been performed for the blade configuration with precone angle $\beta = 5°$. These results are shown in Figure 6 for the quasi-steady aerodynamic models, in Figure 7 for the Loewy-Greenberg formulations, and in Figure 8 for the models based on the BEM solution. For this configuration, all aerodynamic models seem to give results having a similar accuracy, that is quite good for positive values of the collective pitch, but decreases in the negative range of it. This behavior is more evident in the results from the BEM approach, for which a very good accuracy is obtained for positive values of θ, whereas the lead-lag damping seems to be strongly underpredicted for negative values of the collective pitch.

6 Concluding Remarks

The aim of this work has been the definition of different aeroelastic models for the stability analysis of a hovering rotor. Specifically, we have investigated on the importance of inclusion of aerodynamic three-dimensional and unsteady effects on the overall aeroelastic behavior. Both two-dimensional analytical and three-dimensional numerical aerodynamic solutions have been considered. Different approximation techniques for the aerodynamic transfer functions have also been applied. The comparison with experimental results has demonstrated that the inclusion of unsteady effects in the model is essential, in particular for no-precone configurations, and that enhanced accuracy may be obtained by employing a fully three-dimensional model. However, we have also observed that for the problem considered in this work, the aerodynamic transfer functions may be conveniently approximated by a frequency quadratic expression, that seems to be the best combination between accuracy and simplicity of the aeroelastic model. The use if this model could also be convenient for aeroservoelastic applications.

Acknowledgements

This work has been supported by Centro Italiano Ricerche Aerospaziali (C.I.R.A.), grant NR. 007/99: "*Sviluppo di modelli dinamici ed aerodinamici per l'aeroelasticità dei rotori a mozzo non fisso*". The authors wish to thank Dr. L. Flamini and Dr. A. Bassetti for their help in obtaining some of the numerical results presented.

References

1. Loewy, R.G., 'A Two-Dimensional Approximation of Unsteady Aerodynamics of Rotary Wings,' J. of Aeron. Sciences, Vol. 24, (2), 1957.

2. Gaonkar, G.H., and Peters, D.A., 'Review of Dynamic Inflow Modeling for Rotorcraft Flight Dynamics', *Vertica*, Vol. 12, (3), 1988.

3. Kwon, O.J., Hodges, D.H., and Sankar, L.N., Stability of Hingeless Rotor in Hover

Using Three-Dimensional Unsteady Aerodynamics, J. of the American Helicopter Society, 1991.

4. Sharpe, D.L., 'An Experimental Investigation of the Flap-Lag-Torsion Aeroelastic Stability of a Small-Scale Hingeless Helicopter Rotor in Hover,' NASA TP-2546, 1986.

5. Hodges, D.H., and Ormiston, R.A., Stability of Elastic Bending and Torsion of Uniform Cantilever Rotor Blades in Hover with Variable Structural Coupling, NASA TN D-8192, 1976.

6. Hodges, D.H., and Dowell, E.H., Nonlinear Equation of Motion for the Elastic Bending and Torsion of Twisted Nonuniform Rotor Blades, NASA TN D-7818, 1974.

7. Ghiringhelli, G.L., and Mantegazza, P., 'Interpolation Extrapolation and Modeling of Unsteady Linear(ized) Aerodynamic Forces,' *Proceedings of the International Forum on Aeroelasticity and Structural Dynamics*, AAAF, Strasbourg, France, 1993.

8. Johnson, W., Helicopter Theory, Princeton University Press, 1980.

9. Theodorsen, T., 'General Theory of Aerodynamic Instability and the Mechanism of Flutter', NACA Report 496, 1935.

10. Friedmann, P.P, and Yuan, C.H., 'Effect of Modified Aerodynamic Strip Theories on Rotor Blade Aeroelastic Stability,' *AIAA J.*, Vol. 15, (7), 1977.

11. Greenberg, J.M., Airfoil in Sinusoidal Motion in a Pulsating Stream, NACA TN-1326, 1947.

12. Morino, L., 'A General Theory of Unsteady, Compressible, Potential Aerodynamics,' NASA CR-2464, 1974.

13. Morino, L., 'Steady, Oscillatory, and Unsteady Subsonic and Supersonic Aerodynamics - Production Version (SOUSSA - P 1.1) - Volume I - Theoretical Manual,' NASA CR-159130, 1980.

A Matrix-Fraction Approximation

In this appendix we outline the technique adopted for the matrix-fraction of the aerodynamic matrix, E, discussed in Section 4.
The first step in the approximation procedure starts from the observation that in the frequency domain, whatever the model used for the prediction of the aerodynamic loads, their asymptotic behaviors is quadratic, as the frequency tends to infinity. Therefore, following the formulation introduced in Ref. [7], we assume the following form for the matrix-fraction approximation:

$$\mathsf{E}(s) \approx \hat{\mathsf{E}}(s) = s^2 \hat{\mathsf{A}}_2 + s \hat{\mathsf{A}}_1 + \hat{\mathsf{A}}_0 + \left[\sum_{m=0}^{M} \mathsf{D}_m s^m\right]^{-1} \left[\sum_{m=0}^{M-1} \mathsf{R}_m s^m\right] \quad (16)$$

The matrices $\hat{\mathsf{A}}_m, \mathsf{D}_m$ and R_m are real and fully populated (except for D_M that is chosen to be an identity matrix). They are determined by a least-square approximation technique along the imaginary axis. Specifically, the satisfaction of the following condition is required

$$\epsilon^2 = \sum_j w_j \, \mathtt{Tr} \left[\mathsf{Z}^*(s_j) \, \mathsf{Z}(s_j)\right]\Big|_{s_j = ik_j} = \min,$$

where $i = \sqrt{-1}$, w_j denotes a suitable set of weights, and

$$\mathsf{Z}(s) := \left[\sum_{m=0}^{M} \mathsf{D}_m s^m\right] \left[s^2 \hat{\mathsf{A}}_2 + s \hat{\mathsf{A}}_1 + \hat{\mathsf{A}}_0 - \mathsf{E}(s)\right] + \sum_{m=0}^{M-1} \mathsf{R}_m s^m$$

is a measure of the error $(\mathsf{E} - \hat{\mathsf{E}})$.
Next, in order to use the matrix-fraction approximation to determine the time-domain relationship between the aerodynamic loads, f_A, and the state variables, q, equation (16) is recast in the following form

$$\hat{\mathsf{E}}(s) = s^2 \hat{\mathsf{A}}_2 + s \hat{\mathsf{A}}_1 + \hat{\mathsf{A}}_0 + \hat{\mathsf{H}} \left[s\mathsf{I} - \hat{\mathsf{G}}\right]^{-1} \hat{\mathsf{F}}, \quad (17)$$

where $\hat{\mathsf{H}}$ depends upon the R_m's, $\hat{\mathsf{G}}$ upon the D_m's, whereas $\hat{\mathsf{F}}^T = [\mathsf{I}, 0, ..., 0]$ (see Ref. [7] for details). Note that the accuracy of the approximation depends upon the number, M, of matrices used in the matrix-fraction term in equation (16). The appropriate value of M depends upon the characteristics of the functions to be approximated. In our case, these functions corresponds to the elements of the matrix E in terms of the frequency and, for the problem of an hovering rotor, they show a wavy behavior which requires a high value of M (see, *e.g.*, Fig. 1). This, in turn, may induce an instability (*i.e.*, real part greater than zero) in some of the eigenvalues of the matrix $\hat{\mathsf{G}}$ in equation (17); these are spurious poles which are introduced by the interpolation procedure. In order to overcome this problem the iterative procedure of Ref. [7] is adopted. This consists of: (i) diagonalization (or block-diagonalization) of

$\hat{\mathsf{G}}$, (ii) truncation of the unstable states (the matrix $\hat{\mathsf{G}}$ is modified into a smaller matrix G), and (iii) application of an optimal fit iterative procedure to determine new matrices $\mathsf{A}_2, \mathsf{A}_1, \mathsf{A}_0, \mathsf{F}$, and H that replace, respectively, $\hat{\mathsf{A}}_2, \hat{\mathsf{A}}_1, \hat{\mathsf{A}}_0, \hat{\mathsf{F}}$, and $\hat{\mathsf{H}}$ (whereas G remains unchanged throughout the iteration). Hence, the matrix-fraction finite-state approximation assuring a good and stable fit of $\mathsf{E}(s)$ has the final form

$$\hat{\mathsf{E}}(s) = s^2\,\mathsf{A}_2 + s\,\mathsf{A}_1 + \mathsf{A}_0 + \mathsf{H}\,[s\,\mathsf{I} - \mathsf{G}]^{-1}\,\mathsf{F}. \quad (18)$$

B 2–D Aerodynamic Models

For the prediction of unsteady aerodynamic loads acting on hovering rotor blades, a well known analytical model is that presented by Loewy [1], which extends to a rotor-blade section airfoil, the theory introduced by Theodorsen [9] for a fixed-wing section thin airfoil without camber, undergoing plunging and pitching motion, in a constant-velocity free stream. Specifically, the extension of the model consists of including the presence of wake vorticity below the airfoil, in order to simulate, as close as, possible the real flow field generated by a lifting hovering rotor. A more general two-dimensional aerodynamic model may be obtained by following the approach presented in Ref. [10]. There, the correction terms derived by Greenberg [11] for the Theodorsen theory in order to take into account the effects of a pulsating free-stream velocity, have been included in the Loewy formulation, therefore yielding expressions for aerodynamic loads acting on an airfoil having three degrees of freedom in the vertical plane (that in the case of the blade model considered here, correspond to the local values of flapwise bending, chordwise bending, and torsion). Then, this is the analytical model that is applied in this work in order to evaluate the section aerodynamic loadings appearing in the blade structural dynamics equations (1)–(3).
Combining the Loewy formulation with the Greenberg correction, one obtains the following expressions for the section lift and pitching moment about the aerodynamic center

$$\begin{aligned}\mathcal{L} &= 2\pi\rho b\left[\frac{b}{2}(-\dot{\bar{w}} + \bar{v}\dot{\alpha} + \dot{\bar{v}}\alpha + \frac{b}{2}\ddot{\alpha})\right] \\ &\quad + 2\pi\rho b\,\mathcal{C}_{L}(k,\hat{k},h_{w})\,[\bar{v}(-\bar{w} + \bar{v}\alpha + b\dot{\alpha})] \\ \mathcal{M}_{A} &= 2\pi\rho b\left[\frac{b^2}{4}(\dot{\bar{w}} - 2\,\bar{v}\dot{\alpha} - \dot{\bar{v}}\alpha - \frac{b}{2}\ddot{\alpha}) - \frac{b^3}{16}\ddot{\alpha}\right],\end{aligned}$$

where $\bar{v}, \bar{w}$ denote the velocity of the aerodynamic center, respectively parallel (positive aftwards) and perpendicular (positive upwards) to the axis of rotation of the rotor, whereas α is the pith angle of the section (positive nose up). Furthermore, ρ is the air density, b is the airfoil semichord, and $\mathcal{C}_{L}$ is the Loewy's lift deficiency function, depending on the reduced frequency $k = \omega b/\Omega r$, the frequency ratio $\hat{k} = \omega/\Omega$, and the vertical distance between successive rows of vorticity (wake spiral pitch), where ω is the perturbation motion frequency, Ω is the angular velocity of the rotor, and r is the radial distance of the blade section from the hub.
In order to include part of the three-dimensional effects produced by the presence of the tip-vortex (hidden in a two-dimensional model), the model is modified by the inclusion of an induced vertical velocity, v_i. Then, assuming as a first approximation that the lift force is perpendicular to the total velocity, V, and that the skin friction produces a drag force, $\mathcal{D}$ parallel to it, for the aerodynamic forces in equations (1)–(3) we have

$$\begin{aligned}\mathcal{L}_v &= -\mathcal{D} - \gamma\,\mathcal{L} \\ \mathcal{L}_w &= \mathcal{L} - \gamma\,\mathcal{D} \\ \mathcal{M}_\varphi &= \mathcal{M}_{A},\end{aligned}$$

where $\mathcal{D} = b\,\rho\,V^2\,c_{d_0}$, with c_{d_0} denoting the airfoil drag coefficient, and $\gamma \approx v_i/V$. Expressing $\bar{v}, \bar{w}, \alpha$ in terms of the blade elastic displacement variables v, w, φ, and restricting to the steady case, these forces may be used to determine the blade equilibrium configuration. Then, using equations (7)–(9), and linearizing with respect to the perturbation variables, they furnish the equilibrium-dependent aerodynamic transfer function, E.
Note that, due to the presence of the Loewy lift deficiency function, the resulting aerodynamic matrix contains transcendental functions of the frequency and therefore, as described in Section 4, in order to obtain a finite-state aerodynamic operator, it is necessary to apply the matrix-fraction approximation outlined in Appendix A. However, if one introduces the hypothesis of low-frequency approximation for the Loewy lift deficiency function, obtains $\mathcal{C}_{L} \approx 1$, (quasi-steady aerodynamics) and the corresponding aerodynamic matrix contains only polynomial quadratic functions of the frequency. In this case, the aerodynamic generalized forces are defined only in terms of the perturbation modal amplitudes, their first and second time derivative, and the number of aeroelastic eigenvalues is $6N$, and therefore no approximation procedure for the aerodynamic matrix is needed.

C BEM Aerodynamic Model

In this appendix, we outline the algorithm based on a boundary element method (BEM), that we have developed in order to determine an aerodynamic matrix based on a fully three-dimensional unsteady aerodynamic solution.

C.1 Potential Flow Solution

Let us consider an incompressible, inviscid flow, that is initially irrotational. Such a flow field remains irrotational at all times, except for the points which come in contact with the body surface, $\mathcal{S}_B$, since for these points Kelvin's theorem is no longer applicable (there, a contour that remains in the fluid at all times cannot be identified). Indeed, these points form a surface, $\mathcal{S}_W$ (the wake), where vorticity may be different from zero. Hence, if $\mathbf{v}$ denotes the velocity of the fluid particles, it is possible to introduce the potential function ϕ such that $\mathbf{v} = \nabla\phi$ (for $\mathbf{x}$ outside $\mathcal{S}_B \cup \mathcal{S}_W$). Combining the above equation with continuity equation, $\nabla \cdot \mathbf{v} = 0$, one obtains the following Laplace equation

$$\nabla^2\phi = 0 \qquad \text{for } \mathbf{x} \text{ outside } \mathcal{S}_B \cup \mathcal{S}_W .$$

Next, the differential formulation requires the boundary conditions on the body and the wake. The body is assumed to be impermeable, and accordingly the boundary condition on $\mathcal{S}_B$ is $(\mathbf{v} - \mathbf{v}_B) \cdot \mathbf{n} = 0$, where $\mathbf{v}_B$ is the velocity of the points on $\mathcal{S}_B$ and $\mathbf{n}$ is its outward unit normal. Recalling that $\mathbf{v} = \nabla\phi$, one obtains

$$\frac{\partial\phi}{\partial n} = \mathbf{v}_B \cdot \mathbf{n}. \tag{19}$$

The boundary conditions on the wake are obtained from the principles of conservation of mass and momentum across a surface of discontinuity, like $\mathcal{S}_W$. In particular, following the formulation given in Ref. [12], one obtains: (i) $\Delta(\partial\phi/\partial n) = 0$ on the wake surface, and (ii) $\Delta\phi$ =const. following a wake material point.

Starting from this differential formulation and applying the boundary integral equation technique, the frequency-domain potential field solution for a lifting body is expressed by (see Ref. [12] for further details)

$$\begin{aligned}\tilde{\phi}(\mathbf{x}_*) &= \int_{\mathcal{S}_B} \left(\frac{\partial\tilde{\phi}}{\partial n}\, G - \tilde{\phi}\, \frac{\partial G}{\partial n} \right) \mathrm{d}\mathcal{S}(\mathbf{x}) \\ &\quad - \int_{\mathcal{S}_W} \Delta\tilde{\phi}^{TE} \exp(-s\,\tau)\, \frac{\partial G}{\partial n}\, \mathrm{d}\mathcal{S}(\mathbf{x}),\end{aligned} \tag{20}$$

where $G = -1/4\pi\|\mathbf{x} - \mathbf{x}_*\|$ is the unit source solution for the Laplace equation, and τ is the time necessary to convect the material wake point from the trailing edge to the actual position.

The numerical solution of equation (20) has been obtained from its algebraic approximation derived from the discretization of the body and wake surfaces into quadrilateral panels, where $\tilde{\phi}, \partial\tilde{\phi}/\partial n$ and $\Delta\tilde{\phi}$ have been assumed to be constant (zeroth-order boundary-element method). Letting equation (20) be satisfied at the centers of the panels (collocation method), its algebraic approximation assumes the form

$$\begin{aligned}\tilde{\phi}_k &= \sum_{j=1}^{N_B} B_{kj}\tilde{\chi}_j + \sum_{j=1}^{N_B} C_{kj}\tilde{\phi}_j \\ &\quad + \sum_{n=1}^{N_W} F_{kn}\Delta\tilde{\phi}_n^{TE} \exp(-s\tau_n),\end{aligned} \tag{21}$$

where $\chi = \partial\phi/\partial n$. The coefficients appearing in equation (21) are given by

$$B_{kj} = \int_{\mathcal{S}_{B_j}} G_k \,\mathrm{d}\mathcal{S}, \qquad C_{kj} = -\int_{\mathcal{S}_{B_j}} \frac{\partial G_k}{\partial n}\,\mathrm{d}\mathcal{S},$$

$$F_{kn} = -\int_{\mathcal{S}_{W_n}} \frac{\partial G_k}{\partial n}\,\mathrm{d}\mathcal{S},$$

where $G_k = G|_{\mathbf{x}_* = \mathbf{x}_k}$, and $\mathcal{S}_{B_j}$ and $\mathcal{S}_{W_n}$ denote the surfaces of the j-th panel of $\mathcal{S}_B$ and of the n-th panel of $\mathcal{S}_W$, respectively.

Finally, expressing the potential discontinuity at the trailing edge, $\Delta\tilde{\phi}^{TE}$, in terms of the values of the potential at the centers of the body panels, and using equation (21), one obtains the matrix E_2 relating the vector of normalwash at the centers of the panels, v_ϕ, with the vector of potential at the same points,v_χ, *i.e.*, $\tilde{\mathsf{v}}_\phi = \mathsf{E}_2(s)\,\tilde{\mathsf{v}}_\chi$.

C.2 BEM Aerodynamic Matrix

Starting from the potential solution outlined above, in the following we will show that, once the stationary equilibrium configuration has been evaluated (using, for instance, the aerodynamic loads obtained from the potential solution described above, followed by the application of the Bernoulli theorem for determining the pressure), it is possible to define an equilibrium-dependent aerodynamic matrix $\mathsf{E}(\mathsf{q}_0, s)$, by the following expression

$$\begin{aligned}\mathsf{E}(\mathsf{q}_0, s) &= \mathsf{E}_4^I(\mathsf{q}_0)\mathsf{E}_3(\mathsf{q}_0, s)\mathsf{E}_2(\mathsf{q}_0, s)\mathsf{E}_1(\mathsf{q}_0, s) \\ &\quad + \mathsf{E}_4^{II}(\mathsf{q}_0),\end{aligned} \tag{22}$$

where E_1 transforms state variables into blade normalwash (boundary conditions of the potential flow formulation, equation (19)), E_3 transforms the perturbation potential field into perturbation pressure on the body surface, and finally E_4^I and E_4^{II} yield the aerodynamic loads. Note, that the matrix E_2 defined above, when related to the perturbation normalwash, is equilibrium-configuration dependent both through the blade surface deformation that influences coefficients B_{kj}, C_{kj}, and (more important) through the wake surface shape that influences coefficients F_{kn}.

This formulation is a hovering-rotor extension of the fixed-wing formulation of Ref. [13].

C.2.1 Matrix E_1

Let us introduce a set of material curvilinear coordinates, (ξ^1, ξ^2), on the blade surface, and express by $\mathbf{x}(\xi^1, \xi^2, t) = \mathbf{x}_0(\xi^1, \xi^2) + \sum_n q_n(t)\, \mathbf{\Phi}_n(\xi^1, \xi^2)$, the actual position of a surface point in the rotating frame of reference, $\mathbf{x}_0$ being the position of that point in the deformed equilibrium configuration (therefore depending on $q^v_{0n}, q^w_{0n}, q^\varphi_{0n}$, in our problem). Here, $\mathbf{\Phi}_n$ are a set of linearly independent (vector) modes that may be obtained by expressing the deformed blade shape through the beam-theory elastic axis displacements, v, w, φ, combining with equations (4)–(6), and linearizing with respect to the perturbation variables, q. Then, assuming that the origin of the body frame is placed at the center of rotation, and denoting with $\mathbf{\Omega}$ the angular velocity of the rotor, we have

$$\mathbf{v}_{_B}\ (\xi^1, \xi^2, t) = \sum_n \dot{q}(t)\, \mathbf{\Phi}_n(\xi^1, \xi^2)$$
$$+ \quad \mathbf{\Omega} \times \sum_n q_n(t)\, \mathbf{\Phi}_n(\xi^1, \xi^2) + \mathbf{\Omega} \times \mathbf{x}_0(\xi^1, \xi^2).$$

In addition, the unit normal to the body surface has the expression

$$\mathbf{n}(\xi^1, \xi^2, t) = \mathbf{n}_0(\xi^1, \xi^2) + \sum_n q_n(t)\, \boldsymbol{\nu}_n(\xi^1, \xi^2), \quad (23)$$

where $\mathbf{n}_0$ is the unit normal to the equilibrium deformed body surface, whereas $\boldsymbol{\nu}_n$ denotes the variation of $\mathbf{n}$ due to a unit n-th Lagrangean variable, q_n (see Ref. [13], for a detailed description of $\boldsymbol{\nu}_n$).

Next, combining the equations above, and neglecting second-order perturbation terms, the frequency-domain potential-flow boundary condition (normalwash) corresponding to perturbation motion is given by

$$\tilde{\chi} = \sum_n \left[s\, \mathbf{\Phi}_n \cdot \mathbf{n}_0 + \mathbf{\Omega} \times \mathbf{\Phi}_n \cdot \mathbf{n}_0 + \mathbf{\Omega} \times \mathbf{x}_0 \cdot \boldsymbol{\nu}_n \right] \tilde{q}_n,$$

where $\chi = \mathbf{v}_{_B} \cdot \mathbf{n}$.

Finally, dividing the surface of the blade into elements of discretization (panels), and denoting with v_χ the vector containing the values of normalwash, χ_j, at panel centers, the equation above may be recast into the following

$$\tilde{\mathsf{v}}_\chi = \mathsf{E}_1(\mathsf{q}_0, s)\, \tilde{\mathsf{q}},$$

where the generic element (jn) of the matrix E_1 is obtained from

$$E_1^{(jn)}(s) = s\, \mathbf{\Phi}_n(\xi_j^\alpha) \cdot \mathbf{n}_0(\xi_j^\alpha) + \mathbf{\Omega} \times \mathbf{\Phi}_n(\xi_j^\alpha) \cdot \mathbf{n}_0(\xi_j^\alpha)$$
$$+ \mathbf{\Omega} \times \hat{\mathbf{x}}_0(\xi_j^\alpha) \cdot \boldsymbol{\nu}_n(\xi_j^\alpha), \quad \alpha = 1, 2.$$

C.2.2 Matrix E_3

The expression of the matrix E_3 is derived starting from the Bernoulli theorem that, in a frame of reference connected with the blade has the form

$$\frac{\partial \phi}{\partial t} - \mathbf{v}_{_B} \cdot \nabla \phi + \frac{\|\mathbf{v}\|^2}{2} + \frac{p}{\rho} = \frac{p_\infty}{\rho}, \quad (24)$$

where ϕ is the velocity potential, p denotes local pressure, p_∞ is the pressure of the undisturbed flow, $\mathbf{v} = \nabla \phi$, and $\partial / \partial t$ denotes time derivative in blade frame.

Next, set $\phi = \phi_0 + \varphi$ and $p = p_0 + p'$, where ϕ_0 and p_0 denote, respectively, the potential field and the pressure field around the blade in its deformed equilibrium configuration (stationary aerodynamic solution), whereas φ and p' denote, respectively, potential field and pressure field produced by perturbation motion. Equation (24) applied to the aerodynamic solution around the reference configuration yields

$$-\mathbf{v}_{_B} \cdot \nabla \phi_0 + \frac{\|\nabla \phi_0\|^2}{2} + \frac{p_0}{\rho} = \frac{p_\infty}{\rho}. \quad (25)$$

Then, subtracting equation (24) with equation (25), neglecting second-order perturbation terms, and transforming into frequency domain, we obtain the following expression for the pressure perturbation produced by perturbation motion

$$\tilde{p'} = -\rho\, (s\tilde{\varphi} - \mathbf{v}_{_B} \cdot \nabla \tilde{\varphi} + \nabla \phi_0 \cdot \nabla \tilde{\varphi}). \quad (26)$$

Finally, considering the blade discretized into panels, and using dimensionless quantities, equation (26) may be recast in the following matrix form

$$\tilde{\mathsf{p}}' = \mathsf{E}_3(\mathsf{q}_0, s)\, \tilde{\mathsf{v}}_\phi,$$

where E_3 is a matrix operator defined from the discretized form of the gradient operator, and p' is the vector of the perturbation pressure at the centers of the panels.

C.2.3 Matrices E_4^I, E_4^{II}

By definition, for the j-th generalized force induced by perturbation state variables, recalling equation (23) for the expression of the perturbed surface unit normal, we write

$$\tilde{f}_{_{Aj}} = -\int_{\mathcal{S}_{_B}} \left(\tilde{p}'\, \mathbf{n}_0 \cdot \mathbf{\Phi}_j\, \mathrm{d}\mathcal{S} - \tilde{p}_0 \sum_n \tilde{q}_n \boldsymbol{\nu}_n \cdot \mathbf{\Phi}_j \right) \mathrm{d}\mathcal{S}.$$

Then, in matricial form, we have

$$\tilde{\mathsf{f}}_{_A} = \mathsf{E}_4^I\, \tilde{\mathsf{p}}' + \mathsf{E}_4^{II}\, \tilde{\mathsf{q}},$$

where

$$E_4^{I\ (jk)} = \int_{\mathcal{S}_k} \mathbf{n}_0 \cdot \mathbf{\Phi}_j\, \mathrm{d}\mathcal{S},$$

with $\mathcal{S}_k$ denoting the surface of the k-th panel, whereas

$$E_4^{II\ (jn)} = \int_{\mathcal{S}_{_B}} p_0\, \boldsymbol{\nu}_n \cdot \mathbf{\Phi}_j\, \mathrm{d}\mathcal{S}.$$